Aerosol Science and Technology, 43:741–756, 2009

ISSN: 0278-6826 print / 1521-7388 online
DOI: 10.1080/02786820902889879

Stabilization of the Mass Absorption Cross Section of Black Carbon for Filter-Based Absorption Photometry by the use of a Heated Inlet

Y. Kondo,[1] L. Sahu,[1] M. Kuwata,[1] Y. Miyazaki,[2] N. Takegawa,[1] N. Moteki,[1] J. Imaru,[3] S. Han,[1] T. Nakayama,[4] N. T. Kim Oanh,[5] M. Hu,[6] Y. J. Kim,[7] and K. Kita[8]

[1]*Research Center for Advanced Science and Technology, University of Tokyo, Tokyo, Japan*
[2]*Institute of Low Temperature Science, Hokkaido University, Sapporo, Hokkaido, Japan*
[3]*Kanomax Japan, Inc., Suita, Osaka, Japan*
[4]*Solar-Terrestrial Environment Laboratory, Nagoya University, Nagoya, Aichi, Japan*
[5]*Asian Institute of Technology, Klongluang, Pathumthani, Thailand*
[6]*College of Environmental Sciences, Peking University, Beijing, China*
[7]*Advanced Environmental Monitoring Research Center, Gwangju Institute of Science and Technology (GIST), Gwangju, Korea*
[8]*Department of Environmental Science, Graduate School of Science, Ibaraki University, Ibaraki, Japan*

In principle, mass concentrations of black carbon (BC) (M_{BC}) can be estimated by the measurement of the light absorption coefficient of BC. Filter-based methods, which quantify the absorption coefficient (b_{abs}) from the change in transmission through a filter loaded with particles, have been widely used to measure M_{BC}. However, reliable determination of M_{BC} has been very difficult because of the large variability in the mass absorption cross section (C_{abs}), which is the conversion factor from b_{abs} to M_{BC}. Coating of BC by volatile compounds and the co-existence of light-scattering particles contribute to the variability of C_{abs}. In order to overcome this difficulty, volatile aerosol components were removed before collection of BC particles on filters by heating a section of the inlet to 400°C. We made simultaneous measurements of b_{abs} by two types of photometers (Particle Soot Absorption Photometer (PSAP) and Continuous Soot Monitoring System (COSMOS)) together with M_{BC} by an EC-OC analyzer to determine C_{abs} at 6 locations in Asia. C_{abs} was stable at 10.5 ± 0.7 m^2 g^{-1} at a wavelength of 565 nm for BC strongly impacted by emissions from vehicles and biomass burning. The stable C_{abs} value provides a firm basis for its use in estimating M_{BC} by COSMOS and PSAP with an accuracy of about 10%. For the quantitative interpretation of the ratio of the C_{abs} to the model-calculated C^*_{abs}, we measured C_{abs} for monodisperse nigrosin particles in the laboratory. The C_{abs}/C^*_{abs} ratio was 1.4–1.9 at the 100–200 nm diameters, explaining the ratio of 1.8 for ambient BC.

Received 13 October 2008; accepted 10 March 2009.

The authors thank Y. Komazaki, Y. Zhao, D. Kodama, T. Miyakawa, S. Deguchi, M. Fukuda, Y. Morino, M. Nogami, P. Lin, Z. Deng, P. Prapat, and D. T. Canh for their support of the field experiments. We are indebted to the staff of CESS for their cooperation and support in the semi-urban measurements. We thank A. Yamasaki and A. Uchiyama for providing us with the PSAP and nephelometer data obtained in Tokyo and Fukuoka. We also thank Daniel Lack for useful comments. This work was supported by the Ministry of Education, Culture, Sports, Science, and Technology (MEXT), the global environment research fund of the Japanese Ministry of the Environment (B-083), and Asian Pacific Network (APN). This work was partially supported by a KOSEF grant funded by MEST (No. R17-2008-042-01001-0), and the joint research program of the Solar-Terrestrial Environment Laboratory, Nagoya University. L. S. also thanks the Japan Society for the Promotion of Science (JSPS) for a JSPS Research Fellowship for foreign Young Scientists. This study was conducted as a part of the Mega-Cities: Asia Task under the framework of the International Global Atmospheric Chemistry (IGAC) project.

Address correspondence to Y. Kondo, Research Center for Advanced Science and Technology, University of Tokyo, 4-6-1 Komaba, Meguro-ku, Tokyo 153-8904, Japan. E-mail: y.kondo@atmos.rcast.u-tokyo.ac.jp

1. INTRODUCTION

1.1. Variability of the Mass Absorption Cross Section

Black carbon (BC), also referred to as elemental carbon (EC), is produced by incomplete combustion of fossil fuels and biomass. Throughout this article, we use the term BC, which is derived by light absorption, except for cases in which we need to clarify that BC was measured chemically as EC. BC strongly absorbs solar visible radiation and significantly contributes to the radiative forcing of the atmosphere (e.g., Crutzen and Andreae 1990; Ramanathan et al. 2001; 2007; IPCC 2007). BC heats and evaporates clouds, reducing the cloud albedo and thereby warming the surface (Hansen et al. 1997; Ackerman et al. 2000). It can also contribute to climate forcing by changing snow and ice albedos (Warren and Wiscombe 1980; Clarke and Noone 1985; Hansen and Nazarenko 2004). Elevated BC concentrations in

source regions also have deleterious impacts on human health (Lighty et al. 2000). The effects of BC on climate and human health strongly depend on BC concentrations. The temporal and spatial variations of BC are controlled by emissions and transport. Long-term measurements of BC concentrations at various locations close to and distant from sources are very useful for a quantitative understanding of these processes.

Mass concentrations of BC (M_{BC}) can be measured by EC-organic carbon (OC) analyzer based on the thermal-optical-transmittance (TOT) method (e.g., Birch and Carry 1996). More recently, the size distribution and mixing state of BC have been measured with single particle soot photometer (SP2), which is based on laser-induced incandescence (Gao et al. 2007; Moteki and Kondo 2007; 2008). However, it is often difficult to maintain high-quality BC measurement on a long-term basis using these methods, especially at remote sites. M_{BC} can also be estimated by filter based absorption measurement, which is more suitable for continuous observations. Filter-based methods, which quantify the absorption coefficient ($b_{abs}(\lambda)$) at a wavelength of λ from the change in transmission through a filter loaded with particles, have been widely used to estimate M_{BC} because of ease of operation. Mass absorption cross sections $C_{abs}(\lambda)$ [$m^2\ g^{-1}$] need to be determined to convert b_{abs} into M_{BC}. $C_{abs}(\lambda)$ is the absorption cross section per unit BC mass and is also known as the mass absorption coefficient or mass absorption efficiency. Values of $C_{abs}(\lambda)$, however, have been observed to vary by a large factor even for the same wavelength. Enhanced absorption due to internal mixing of BC particles is considered to cause significant variability in $C_{abs}(\lambda)$ (e.g., Liousse et al. 1993; Petzold et al. 1997; Martins et al. 1998; Reid et al. 1998; Hitzenberger et al. 1999; Sharma et al. 2002; Sheridan et al. 2005; Chou et al. 2005; Bond and Bergstrom 2006 and references therein; Zhang et al. 2008). The variability in $C_{abs}(\lambda)$ still remains the most important and difficult issue that needs to be overcome in accurately deriving M_{BC} from b_{abs} (Slowik et al. 2007; Taha et al. 2007; Cappa et al. 2008; Lack et al. 2008).

1.2. Corrections Required for Filter-Based Absorption Coefficient

The absorption coefficient of airborne BC particles is defined from the Beer-Lambert law and is expressed as

$$b^*_{abs}(\lambda) = \int \sigma^*_{abs}(D_{BC}, \lambda)(dN_{BC}/d\log D_{BC})\ d\log D_{BC} = \int [\sigma^*_{abs}(D_{BC}, \lambda)/(\rho_{BC}\pi D^3_{BC}/6)] \times (dM_{BC}/d\log D_{BC})\ d\log D_{BC}, \quad [1]$$

where $dN_{BC}/d\log D_{BC}$ and $dM_{BC}/d\log D_{BC}$ are the number and mass size distributions, respectively, as a function of BC core diameter (D_{BC}). $\sigma^*_{abs}(D_{BC}, \lambda)$ is the absorption cross section [m^2] per particle. M_{BC} is expressed as

$$M_{BC} = \int \rho_{BC}\ (\pi D^3_{BC}/6)(dN_{BC}/d\log D_{BC})d\log D_{BC}, \quad [2]$$

where ρ_{BC} is the BC density.

The mass absorption cross section of airborne BC ($C^*_{abs}(\lambda)$) is defined as

$$C^*_{abs}(\lambda) = b^*_{abs}(\lambda)/M_{BC}. \quad [3]$$

The absorption coefficients of BC deposited on filters ($b_{abs}(\lambda)$) and the corresponding mass absorption cross section ($C_{abs}(\lambda)$) are different from $b^*_{abs}(\lambda)$ and $C^*_{abs}(\lambda)$, as discussed in detail below.

Operationally, the absorption coefficients are determined by filter-based absorption photometers by the following equation:

$$b_0(\lambda) = (A/V)\ln[I_{t-\Delta t}(\lambda)/I_t(\lambda)] \quad [4]$$

where A is the area of the sample spot, V is the air sample volume during a given time period Δt (between t-Δt and t), and $I_{t-\Delta t}$ and I_t are the average transmittances (Bond et al. 1999). It is well known that $b_0(\lambda)$ can be quite different from the $b^*_{abs}(\lambda)$ defined by Equation (1). Correction factors have been introduced to convert $b_0(\lambda)$ to obtain $b_{abs}(\lambda)$:

$$b_{abs}(\lambda) = f_{fil} f_{amp}\, b_0(\lambda), \quad [5]$$

where f_{fil} represents the magnification of absorption by multiple scattering in the filter media. f_{fil} varies with the aerosol penetration depth into the filter and therefore can depend on aerosol size, face velocity, properties of the filter matrix, and the details of the optical arrangement. f_{amp} represents the amplification of light absorption of BC depending on its mixing state.

For f_{fil}, the following equation has been used and evaluated by laboratory and field experiments using a particle soot absorption photometer (PSAP, Radiance Research, Seattle, WA, USA) for poly-disperse BC with diameters less than 1 μm (Bond et al. 1999),

$$f_{fil} = [1/(1.0796\,Tr + 0.71)]/1.22, \quad [6]$$

where, Tr ($= I_t/I_{t=0}$) is the filter transmission. The f_{fil} determined by different methods (e.g., Bond et al. 1999; Virkkula et al. 2005) differ only by about 6%. We have used Equation (6) throughout the present study. The uncertainty in using this equation is discussed in section 6.

f_{amp} includes the effect of BC coating by non-absorbing compounds and the co-existence of non-absorbing particles, which are all embedded in the filter. There exists no analytical formulation that represents f_{amp} for different mixing states of BC embedded in filter media, although calculations of this effect for airborne BC particles have been made (e.g., Horvath 1997;

Fuller et al. 1999; Schnaiter et al. 2005; Mikhailov et al. 2006; Bond and Bergstrom 2006 and references therein). f_{amp} was reported to vary by as much as a factor of 2–3, depending on the coating thickness of BC. Throughout this study, f_{amp} was set to 1 for the analysis of the photometer data. This assumption does not introduce any additional uncertainty in the conclusions.

In order to minimize the variability in $C_{abs}(\lambda)$, we have developed a technique to remove volatile aerosol components using an inlet heated to 400°C, as discussed in detail in sections that follow. First, the volatility of different chemical components of aerosols and the transmission efficiency of BC through the heated inlet were evaluated. Second, we compared the variability in $C_{abs}(\lambda)$ obtained using the heated inlet with that for an unheated inlet. We derived $C_{abs}(\lambda)$ using simultaneously measured $b_{abs}(\lambda)$ and M_{BC},

$$C_{abs}(\lambda) = b_{abs}(\lambda)/M_{BC}. \quad [7]$$

We show that the variability in $C_{abs}(\lambda)$ for the heated inlet measured at different locations in Asia was small enough to enable accurate measurements of M_{BC} from light absorption by BC in the fine mode.

2. PHOTOMETERS

For the measurement of $b_{abs}(\lambda)$, we used two types of photometers: single-wavelength PSAP ($\lambda = 565$ nm) and Continuous Soot Monitoring System (COSMOS, Kanomax, Osaka, Japan) (Miyazaki et al. 2008). The configurations of optics and filter mounting parts of the PSAP and COSMOS are compared in Figure 1.

Throughout the present study, we did not make any correction of the effect of scattering by aerosols collected on the filter in deriving $b_{abs}(\lambda)$ because of the lack of scattering data. The correction is represented by the term $s \times b_{scat}$, where b_{scat} and s are the scattering coefficient of non-absorbing aerosol and scattering correction factor (Bond et al. 1999; Virkkula et al. 2005). The value of s has been estimated to be 0.016 ($= 0.02/1.22$) $\pm$ 0.016 (Bond et al. 1999). This may result in some overestimation of $b_{abs}(\lambda)$ for the data obtained using an unheated inlet. The degree of overestimation is discussed in section 5.1. On the other hand, by using a heated inlet, almost all the light-scattering aerosols are evaporated, resulting in a smaller scattering correction than for direct ambient measurement. Despite the uncertainty of the correction for scattering, comparison of $b_{abs}(\lambda)$ obtained with unheated and heated inlets provides useful information.

2.1. PSAP

For PSAP measurements, particles are collected on a glass-fiber filter (Pallflex E70-2075W, Pall, USA) with typical sample flow rates of 0.5–0.7 STP (@ 0°C and 1013 hPa) liter min^{-1}. The transmission of light through the filter was measured at a wavelength of 565 nm. The attenuation of light through the filter was converted to absorption coefficient, including the corrections based on Equation (6). The temperatures of the filter cartridges and photo detectors were maintained at 40°C to prevent possible moisture condensation in the sample air (Arnott et al. 2003). The limit of detection (LOD) for S/N = 2 was measured to be 1 Mm^{-1} (about 0.1 μg m^{-3}) for a 10-minute integration time (Miyazaki et al. 2008). A more-detailed analysis of the noise characteristics of the PSAP has been made by Springston and Sedlacek (2007). According to Bond et al. (1999), filter-loading correction for the PSAP is not recommended when the Tr value falls below 0.7. Therefore, the transmittance value

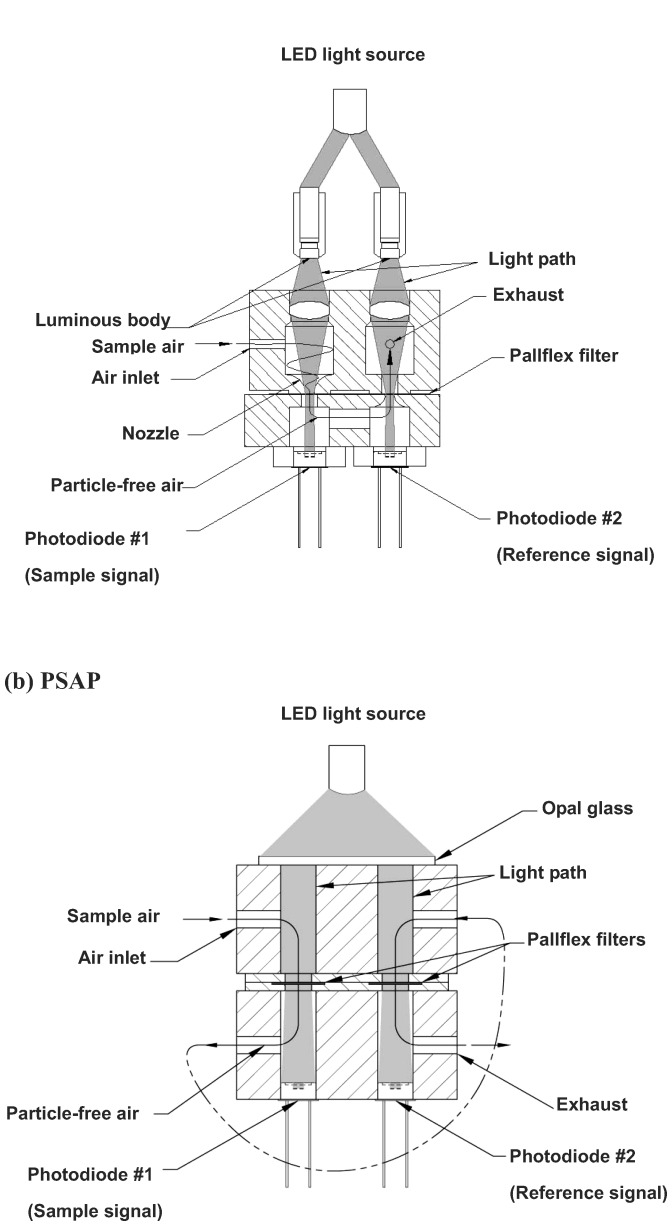

FIG. 1. Optical and filter mounting parts of COSMOS and PSAP.

criterion for changing the filter was set at $Tr = 0.7$. The sample flow (V in Equation [4]) and sample spot area (A) were measured with accuracies of 1% and 2%, respectively.

2.2. COSMOS

COSMOS is designed for fully automated, high-sensitivity, and continuous measurement of $b_{abs}(\lambda)$. The aerosol is collected on a quartz-fiber filter at typical flow rates of 0.5–0.7 STP liter min^{-1}. The flow rate of the sample air is controlled by a mass flow controller to ensure constancy and long-term repeatability under varying conditions. The sample collecting spot area of COSMOS is 18.1 mm^2, which is similar to the 19.6 mm^2 area for PSAP. The material of the quartz-fiber filter used for COSMOS is the same as that used for PSAP (Pallflex E70-2075W, Pall, USA). This enables the use of the same f_{fil} for COSMOS and PSAP. COSMOS uses a roll of 40 mm wide filter tape, which is automatically advanced when the filter transmittance decreases to a pre-set value, typically 0.7.

Light from the high-intensity light-emitting diode (LED) at a wavelength of 565 nm is first focused by a double-convex (DCX) lens (Edmund Optics, Barrington, NJ, USA) and is then directed and split equally by optical fibers (Figure 1). The light passing through the two optical bundle pipes is again focused by DCX lenses before being directed toward the filter in order to maximize the photon flux. The photon fluxes transmitted through the filter are detected by silicon photodiodes (S2386-45K, Hamamatsu Photonics, Hamamatsu, Japan) with an active area of 3.9 × 4.6 mm^2. The light signals are digitized at a frequency of 1000 Hz with a resolution of 20 bits and are averaged over 1 min.

PSAP is known to show erroneously high light absorption associated with rapid humidity changes due to corresponding changes in the physical characteristics of its filters (Arnot et al. 2003). The temperatures of the optical detector unit and filter holding unit of COSMOS are actively maintained at 50°C to minimize any possible effects of changes in ambient relative humidity. In addition, the sample air, after passing through the filter from above, is then passed through the reference section of the filter, resulting in the same air composition for the sample and reference units. Aircraft measurements of 1 min averaged absorption coefficients by COSMOS made over the East China Sea in spring 2008 showed very stable values under varying humidity.

The $b_{abs}(\lambda)$ values were obtained by applying the same correction factor f_{fil} as for PSAP. The LOD for the current version of COSMOS for S/N = 2 was determined to be about 0.15 Mm^{-1} (about 0.015 μg m^{-3}) for a 10 min integration time. The high data acquisition frequency, reduction of noise, and the high photon flux lead to the low LOD. The $b_{abs}(\lambda)$ values obtained measured by PSAP and COSMOS were highly correlated ($r^2 = 0.97$), with a linear regression slope of 0.97 ± 0.01 during a 9 day intercomparison made in Tokyo (Miyazaki et al. 2008). Within the 95% confidence interval, the linear regression fit suggested no biases between the $b_{abs}(\lambda)$ values measured by the two instruments.

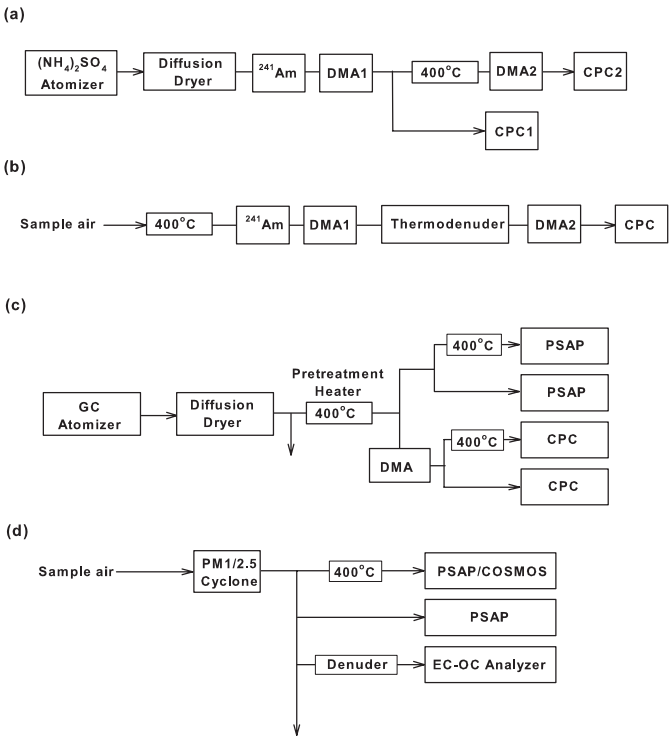

FIG. 2. Instrumental setup for (a) measurement of volatility of $(NH_4)_2SO_4$ in the laboratory using differential mobility analyzers (DMAs) and condensation particle counters (CPCs), (b) assessment of the effect of re-condensation using ambient aerosol, (c) laboratory measurement of glassy carbon (GC) particle losses through a heated inlet, and (d) air sampling configuration for the measurements of absorption coefficients by the PSAP/COSMOS and EC-OC instruments.

3. HEATED INLET

3.1. Design and Performance Tests

Relatively volatile aerosol components were removed by heating the inlet. The overall configuration of measurements of the performance of the heated inlet using the PSAP is shown in Figures 2a–c. Stainless steel (SUS316) tubes with 3/8 inch outer diameters and 0.049 inch thick were used as the air-sampling inlet. A section of about 21 cm of the inlet line was heated to a predefined temperature using an electric jacket heater (Type PK, Tokyo Technological Laboratory, Japan). The inlet temperature was regulated by a temperature controller (E5GN, Omron, Japan) using a thermocouple mounted on the outer surface of the central part of the heated stainless steel tube. The residence time of the particles in the section heated at 400°C is about 0.3 s for the sample flow rate of 0.7 STP liter min^{-1}. The air samples were then cooled down to ambient conditions by passing them through a 1 m long stainless steel (SUS316) tube before measurement.

The volatilization characteristics of the heater were measured by both laboratory experiments and atmospheric observations. $(NH_4)_2SO_4$ particles were generated from aqueous solution of the compounds using an atomizer (Model 3076, TSI, St. Paul, MN, USA) in the laboratory (Figure 2a). The generated particles were dried using two diffusion dryers (Model 3062, TSI) and size-selected (30, 50, 100, and 200 nm) by a differential mobility analyzer (DMA, Model 3081, TSI). $(NH_4)_2SO_4$ started to evaporate at 150°C, irrespective of the particle size. Particles with diameters smaller than 100 nm completely evaporated at 200°C. At 200 nm, complete evaporation occurred at 225°C. The present result generally agrees well with previous studies (Villani et al. 2007; Paulsen et al. 2006; Philippin et al. 2004; Pinnick et al. 1987; Clarke et al. 1987).

The performance of the heated inlet was also measured for ambient aerosols in Tokyo in June 2004. The heated inlet was placed between the inlet sample manifold and an Aerodyne quadrupole aerosol mass spectrometer (Q-AMS) (Aerodyne Research, USA) (Jayne et al. 2000; Takegawa et al. 2005) with a 2 min time resolution. The vaporizer of the Q-AMS was heated to 600°C. The inlet was heated up to ~500°C and passively cooled down to room temperature (25°C). During this experiment, the aerosol mass concentration was stable at 39 ± 3 μg m^{-3}. The ambient concentrations of organics, SO_4^{2-}, NO_3^-, and NH_4^+ were 14.4, 3.4, 5.7, and 6.1 μg m^{-3}, respectively. Figure 3 shows the relationships between the mass of the volatile components and heater temperature (30°–480°C). The 50% (90%) evaporation temperatures of organic aerosol (OA), SO_4^{2-}, NO_3^-, and NH_4^+ were approximately 120 (300)°C, 200 (250)°C, 80 (120)°C, and 80 (120)°C, respectively. The 50–90% volatilization temperatures for SO_4^{2-} (200°–250°C) are similar to those measured in the laboratory (200°–225°C). The analysis of Q-AMS mass spectra indicates that the evaporative NO_3^- at 250°–400°C originates from $NaNO_3$. The volatile components evaporated almost completely at 400°C. The present results are consistent with aerosol volatility measurements using a thermodenuder (Huffman et al. 2008). These results also indicates little interference of re-condensation for the discussion of aerosol mass concentrations.

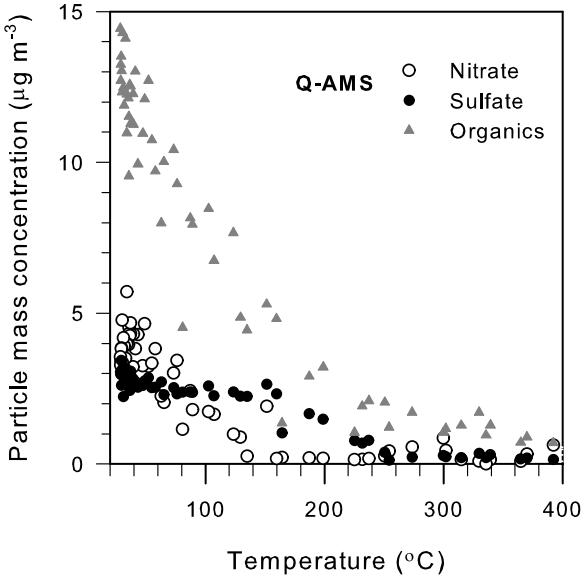

FIG. 3. Mass concentrations of major inorganic (SO_4^{2-}, NO_3^-, and NH_4^+) and organic aerosol components as a function of inlet temperature measured by the Q-AMS.

For further confirmation, the effect of re-condensation of the volatilized species was assessed by using the experimental setup shown in Figure 2b. Ambient particles with diameters of 50, 100, 200, and 300 nm were passed through the inlet section heated at 400°C to extract non-volatile cores, which were size-selected by DMA1. Then, these non-volatile cores were reheated to 400°C in a thermodenuder (Model 3065, TSI), followed by size measurement by DMA2. No detectable changes in particle size due to re-heating were observed, suggesting no significant effect of re-condensation.

The transmission efficiency of BC through the heated inlet can be influenced by particle diffusion and thermophoretic losses depending on size and temperature (Philippin et al. 2004). The transmission efficiency of the BC particles through our heated inlet was measured by the system shown in Figure 2c. Glassy carbon (GC) (Tokai Carbon, Japan) particles in an aqueous suspension were generated by an atomizer, dried with a diffusion drier, and heated to 400°C to remove the volatile compounds. The $b_{abs}(\lambda)$ values for GC were monitored by the PSAPs with and without a heated inlet. The mono-modal GC particles (with mobility diameters of 30, 45, 60, 75, 100, and 150 nm) were size-selected using the DMA. The diameters of the generated GC (D_{BC}), measured with the DMA + CPC system, ranged from 10 to 800 nm, with a peak around 100 nm. The linear regression of the $b_{abs}(\lambda)$ values measured by the two PSAPs exhibited a high correlation ($r^2 = 0.94$), with a slope of 1.0. No detectable loss of GC was observed for D_{BC} = 100–150 nm, although 2–5% loss was observed at D_{BC} = 30–75 nm. We also measured the transmission of sodium chloride (NaCl) particles with diameters of 20–300 nm, which are also non-volatile at 400°C. The transmittance of NaCl through the heated inlet was 0.98 ± 0.01.

3.2. Non-Volatile Aerosol Component

The total mass concentrations of non-volatile cores of aerosols extracted by the same heated inlet were compared with the simultaneously measured M_{BC} by a semi-continuous EC-OC analyzer (Sunset Laboratory, Tigard, OR) in Tokyo (Kondo et al. 2006). For the M_{BC} measurements, the air sample was introduced into a cyclone with a 50 % effective cut-off diameter of 2.5 μm to reject coarse particles at 16.7 liter min^{-1}. Ambient aerosol was collected on a quartz-fiber filter (2500QAT, Pall) for 45 min at a sample flow rate of 8 liter min^{-1}. A parallel-plate carbon filter denuder was installed to remove volatile species. Then during the next 15 min, the samples were analyzed for

M_{BC}. EC was converted to CO_2 and determined using a non-dispersive infrared (NDIR) detector. The protocols prescribed by the National Institute for Occupational Safety and Health (NIOSH) (Birch and Cary 1996) were applied to the EC measurements. The LOD for these measurements was estimated to be 0.4 μg m^{-3} from the variability of the zero level (2σ). In addition to this error, uncertainties of the EC-to-OC split, which may depend on temperature protocol, can lead to an overall accuracy of 22% (Kondo et al. 2006).

The mass concentrations of non-volatile cores and M_{BC} agreed to within 10% with a slope of 0.96 in Tokyo (Kondo et al. 2006). This means that we can directly relate BC mass concentration with $b_{abs}(\lambda)$ measured by a photometer with a heated inlet. Charring of organic compounds occurs primarily for polar organics and becomes significant at temperatures above 430°C (Yu et al. 2002). The present measurement shows that charring has insignificant effects in extracting BC mass using the heated inlet with a residence time of 0.3 s.

Light-absorbing dust particles or the oxidation catalysts of alkaline metals and sea salts are the potential causes of interferences (Novakov and Corrigan 1995; Yu et al. 2002). These particles are distributed mainly in the coarse mode. We applied the heating technique to the measurement of BC in fine particles to minimize the effect of light-absorbing particles other than BC.

4. CALCULATED MASS ABSORPTION CROSS SECTION

By using the heated inlet, $\sigma^*_{abs}(D_{BC}, \lambda)$ should not depend on the mixing state of BC. However, $C^*_{abs}(\lambda)$ may vary depending on the refractive index, shape of particles, and size distribution of BC, according to Equation (1). The size dependent mass absorption cross section, $\sigma^*_{abs}(D_{BC}, \lambda)/(\rho_{BC}\pi D^3_{BC}/6)$, was calculated for complex refractive indices of $n = 1.75 - 0.63$i and 1.95 – 0.79i at 565 nm. It reached a maximum value of 6–7 m^2 g^{-1} at D_{BC} of about 170 nm, similarly to that shown by Bond and Bergstrom (2006). Here we assumed that BC particles are spherical and $\rho_{BC} = 1.8$ g cm^{-3}. $C^*_{abs}(\lambda)$ was calculated using $\sigma^*_{abs}(D_{BC}, \lambda)/(\rho_{BC}\pi D^3_{BC}/6)$ and assuming lognormal BC size distributions with mass median diameters of 100–300 nm and $\sigma = 1.6$. $C^*_{abs}(\lambda)$ gradually decreased from about 5.7 ± 0.3 m^2 g^{-1}at $D_{BC} = 100$–150 nm to 4.4 ± 0.2 m^2 g^{-1} at 300 nm.

The major mass fraction of BC in urban plumes in Japan and the United States was in the range of 100 to 500 nm peaking at around 180 nm (Kondo et al. 2006; Moteki et al. 2007; Schwarz et al. 2008). In addition, measurements of the size distributions were made by a SP2 (Shiraiwa et al. 2008) at Fukue Island (32.8°N, 128.7°E) in Japan in spring 2007. The mass size distributions of BC strongly impacted by emissions from northeastern China, Korea, and Japan were more or less similar with mass median diameters of 200–220 nm. The size of BC from biomass burning was observed to be somewhat larger than that emitted in urban areas (mainly vehicular emissions) (Schwarz et al. 2008). The calculations based on Mie theory suggest that the change in the BC size distributions will not change $C^*_{abs}(\lambda)$ more than 10% for these size distributions.

In general, fresh BC particles emitted into the atmosphere are not spherical but are agglomerates of primary spherules (Bond and Bergstrom 2006). Refractive indices of atmospheric BC are not fully understood. In addition, $C_{abs}(\lambda)$ for BC particles collected on filters can be different from those for airborne particles due to multiple reflections, as represented by f_{fil}. These factors introduce uncertainties in the absolute values of $C_{abs}(\lambda)$ even for the heated inlet. Therefore we need to measure $C_{abs}(\lambda)$ and its variability by atmospheric measurements, as described in the next section.

5. MEASUREMENTS OF THE MASS ABSORPTION CROSS SECTION

5.1. Ambient Measurements of b_{abs} and M_{BC}

We made measurements of $b_{abs}(\lambda)$ by using PSAP or COSMOS simultaneously with in situ measurements of M_{BC} to determine $C_{abs}(\lambda)$ using the set up shown in Figure 2d. The measurements were made at two sites in the Tokyo Metropolitan Area (TMA) in Japan, on Jeju Island in Korea, at rural sites near Guangzhou and Beijing in China, and in Bangkok in Thailand in different seasons as shown in Figure 4 and summarized in Table 1. Hereafter, the sample volumes in deriving $b_{abs}(\lambda)$ (Equation [4]) and M_{BC} were normalized to those at 25°C and 1013 hPa. The air sample was introduced into a cyclone with a 50% effective cut-off diameter of 2.5 μm ($PM_{2.5}$) or 1 μm (PM_1) to exclude coarse particles. Figure 5 shows the time series of $b_{abs}(\lambda)$ and M_{BC} in Tokyo. Generally, $b_{abs}(\lambda)$ and M_{BC} showed large ranges of variations, with well-correlated temporal trends at all sites. Below, we discuss important sources and the typical mixing state of BC at each site. The ratios of OOA/SO_4^{2-}, OOA/M_{BC}, SO_4^{2-}/M_{BC}, and D_p/D_{BC}

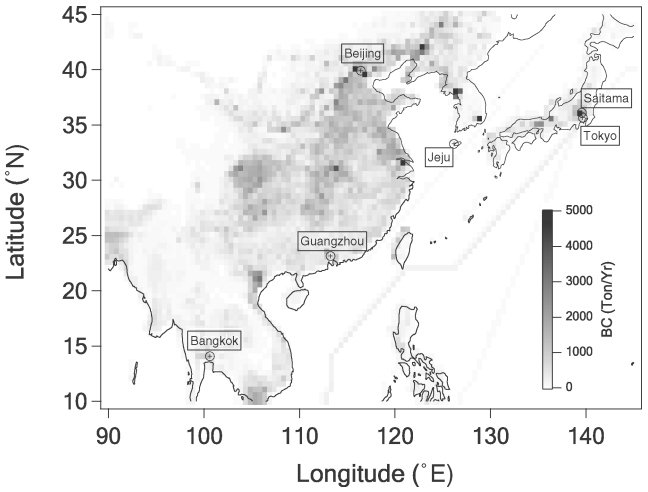

FIG. 4. Map of the site of the measurements of the absorption coefficients and BC mass concentrations. Distributions of anthropogenic emissions of BC for the year 2000 at 0.5° × 0.5° resolution (Streets et al. 2003) are also shown.

TABLE 1
Locations and periods of measurements of absorption coefficients and BC mass concentrations. The types of photometers and EC concentrations are also shown

Location	Period	Instrument/Method	M_{BC} (μg m^{-3})					
Urban Tokyo, RCAST in Komaba, Japan 35.7°N, 139.7°E	July–August 2004	Heated-PSAP Unheated-PSAP Sunset semi-continuous	Median	Mean	S. D.	Max.	Min.	(n)
				(July–August)				
			1.43	1.68	1.02	7.13	0.21	(559)
				(November–December)				
			2.6	23.34	2.40	15.30	0.30	(609)
Suburban Saitama CESS in Kisai, Japan 36.1°N, 139.6°E	July–August 2004	Heated-PSAP Filter Sampling/ TOT		(July–August)				
			2.07	2.27	1.22	6.43	0.14	(78)
Remote Jeju Island Gosan, Korea 33.2°N, 126.1°E	March–April 2005	Heated-PSAP Unheated-PSAP Sunset semi-continuous		(March–April)				
			0.86	1.17	0.88	4.15	0.05	(421)
Rural Guangzhou, China 23.5° N, 113.0°E	July 2006	Heated-PSAP Unheated-PSAP Sunset semi-continuous		(July)				
			2.83	4.30	5.35	56.1	0.38	(483)
Rural Beijing, China 39.52°N, 116.30°E	August 2006	Heated-PSAP Unheated-PSAP Sunset-semi continuous		(August)				
			3.70	3.90	2.20	10.4	0.6	(60)
Suburban Bangkok, Thailand 14.1°N, 100.6°E	July–August November–December 2007	Heated-COSMOS Sunset semi-continuous		(July–August)				
			2.26	2.97	2.6	48.0	0.05	(480)
				(November–December)				
			4.04	4.84	2.92	21.3	1.08	(300)

in the TMA and at Gosan estimated by combining the measurements at these sites (Kondo et al. 2007; Shiraiwa et al. 2007; Miyazaki et al. 2007; Kuwata et al. 2007; Kuwata and Kondo 2008; Miyakawa et al. 2008; Sahu et al. 2009) are summarized in Table 2. Here OOA (nearly equivalent to SOA) and D_p represent oxygenated organic aerosol and particle diameter, respectively.

Measurements at the Research Center for Advanced Science and Technology (RCAST) of the University of Tokyo were conducted in the summer of 2004 (Kondo et al. 2008). Major sources of BC in Tokyo have been estimated to be dominated by emissions from diesel vehicles (Kondo et al. 2006). The representative data of the fresh and aged air masses at this location are shown in Table 2. Measurements were also made at the Center

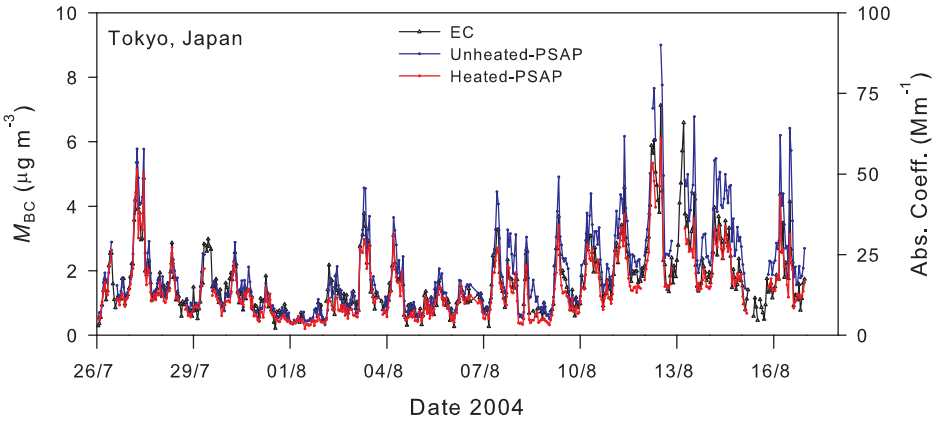

FIG. 5. Time series of the light absorption coefficients and BC mass concentrations at RCAST in Tokyo, Japan.

TABLE 2
Average aerosol chemical composition in Tokyo, Kisai (Saitama), and Gosan

	Tokyo fresh	Tokyo aged	Kisai very-aged	Gosan
OOA/SO_4^{2-}	1.2	1.5	2.0	1.0
OOA/M_{BC}	2.6	4.2	6.4	2.8
SO_4^{2-}/M_{BC}	2.2	2.9	2.9	2.8
D_p/D_{BC}	1.05	1.3	N/A	1.6*

*The value was obtained with a volatility tandem differential mobility analyzer in spring 2005.

for Environmental Science (CESS) in Kisai city, Saitama prefecture in the TMA, located about 50 km north of Tokyo. Kisai is downwind of Tokyo during the daytime in summer because of sea breezes. The aged and very aged air masses in Table 2 were measured at this location.

The measurements at Gosan on Jeju Island, Korea, were made in the spring of 2005. This site is located in the East China Sea ~100 km south of the Korean mainland, ~250 km west of Kyushu, Japan, ~500 km east-northeast of Shanghai, China, and was often impacted by the outflow from China and Korea. The $b_{abs}(\lambda)$ and M_{BC} were high in the outflow from China and Korea, while they were much lower in maritime air. The D_p/D_{BC} ratios at Gosan were much higher than fresh and aged air in Tokyo.

We made measurements at Backgarden, a small village in a rural farming environment on the outskirts of the densely populated center of the Pearl River Delta (PRD), China in the summer of 2006. The Backgarden site is located about 60 km northwest of Guangzhou city (Garland et al. 2008). At this site, the range of variations in M_{BC} was largest (0.4–56 μg m^{-3}). The sources of BC at this site are not well understood, although transport from Guangzhou is likely important. M_{BC} reached its highest values during the nighttime under calm wind conditions, when local burning was the major source.

Measurements were also conducted at Yufa in August 2006. The site is located in a rural area about 50 km south of Beijing (Takegawa et al. 2008). A major highway is located ~1.2 km east of this site. BC often increased during the nighttime, similarly to the urban center of Beijing, where the BC concentrations were strongly influenced by exhaust from diesel vehicles (Han et al. 2008). It is likely that BC at Yufa was also strongly influenced by fresh emissions from diesel vehicles.

The measurements of $b_{abs}(\lambda)$ at the Asian Institute of Technology (AIT) were made by an automated COSMOS instrument in 2007–2008. AIT is located about 40 km north from the main city center of Bangkok, Thailand. The campus of AIT is along the west side of the Phahonyothin road, which is a major pathway connecting the north-northeastern sector to the center of Bangkok (Kim Oanh et al. 2000).

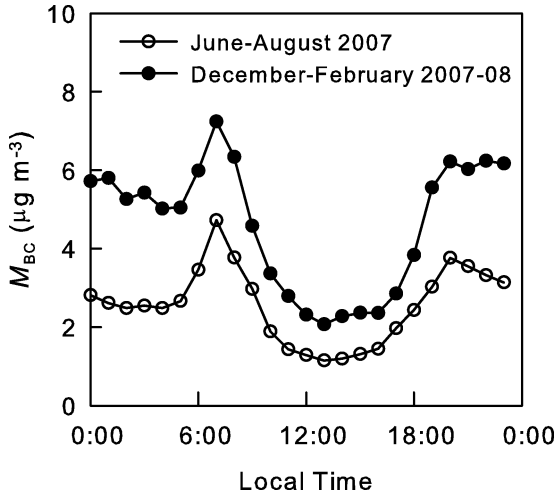

FIG. 6. Diurnal variations of median BC concentrations measured at AIT in Bangkok, Thailand, in summer and winter.

The heavy traffic is composed of gasoline- and diesel-fueled vehicles.

The BC sources in Bangkok varied depending on season. In the rainy season (May–October), the BC at AIT was dominantly influenced by vehicular emissions. Generally in Thailand, particularly in the dry season (November–April), the open burning of biomass and agricultural waste are important sources of carbonaceous aerosols (BC and organic aerosol). At AIT, M_{BC} and OC concentrations and OC/M_{BC} ratios were considerably higher in the dry season than those in the rainy season. The median diurnal-seasonal variations of M_{BC} clearly show the effect of biomass burning on BC in December–February as compared with June–August, as shown in Figure 6.

In addition to the above measurements, $b_{abs}(\lambda)$ and b_{scat} were measured simultaneously using a PSAP with an unheated inlet and a nephelometer (Model 3563, TSI) in Tokyo between August and September in 2007 and in Fukuoka (33.6°N, 130.4°E) in Kyushu, Japan, between March and May in 2008 (A. Yamasaki, A. Uchiyama, T. Nakayama, and Y. Matsumi, unpublished data). Aerosol samplings were made without size segregation. PSAP filters were routinely replaced three times per day and more frequently at higher aerosol loadings. Fukuoka is located about 360 km east of Gosan and was also influenced by the Asian outflow in spring. The average $b_{abs}(\lambda)$ in Fukuoka was similar to that at Gosan. The average (median) $\pm 1\sigma$ corrections of scattering ($s \times b_{scat}$) to $b_{abs}(\lambda)$ were 14.1(14.1) $\pm$ 4.9% and 15.7(13.3) $\pm$ 9.3% for Tokyo and Fukuoka, respectively, suggesting that $b_{abs}(\lambda)$ measured using an unheated inlet in Tokyo and at Gosan were overestimated by about 15%.

5.2. Estimates of the Mass Absorption Cross Section

Figure 7 shows correlations between $b_{abs}(\lambda)$ and M_{BC} measured in Tokyo, corresponding to the time series shown in section 5.1. We used bivariate regression analysis incorporating

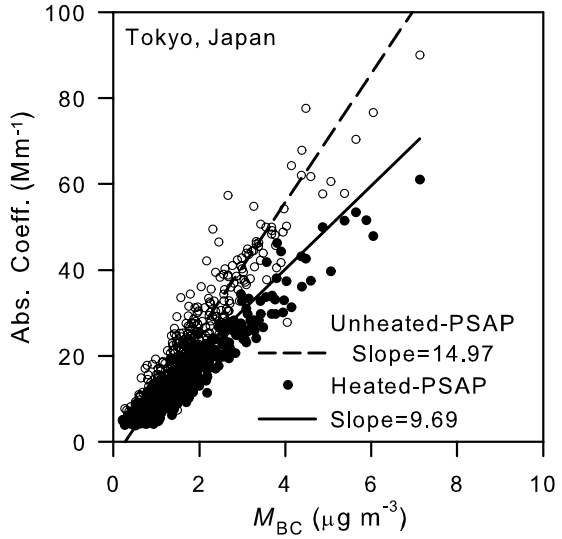

FIG. 7. Correlation plots of the light absorption coefficient versus the BC mass concentration at RCAST in Tokyo, Japan.

the errors in both variables. Table 3 summarizes the statistics, including the regression slope and correlation coefficients, obtained from the relationships between $b_{abs}(\lambda)$ and M_{BC} at all sites. Overall, $b_{abs}(\lambda)$ and M_{BC} were correlated well for heated ($r^2 = 0.87$–0.98) and unheated inlets ($r^2 = 0.80$–0.96). Because of the high correlations between $b_{abs}(\lambda)$ and M_{BC}, the slope of the correlation gives $C_{abs}(\lambda)$ for unheated (unheated-$C_{abs}(\lambda)$) and heated inlets (heated-$C_{abs}(\lambda)$).

The unheated-$C_{abs}(\lambda)$ showed a larger variability (about 40%) than heated-$C_{abs}(\lambda)$ (about 10%). The unheated-$C_{abs}(\lambda)$/heated-$C_{abs}(\lambda)$ ratios ranged between 1.2 and 1.6. Recent laboratory and field measurements have shown that the presence of secondary organic aerosol (SOA), in an external mixture can cause an increase in the light absorption measured by filter-based photometers (Cappa et al. 2008; Lack et al. 2008). For the analysis of the relationship of the unheated-$C_{abs}(\lambda)$ with OA, the unheated-$b_{abs}(\lambda)$/heated-$b_{abs}(\lambda)$ ratios are plotted versus the OC/M_{BC} ratio in Figure 8.

It is seen that in Tokyo, the unheated-$b_{abs}(\lambda)$/heated-$b_{abs}(\lambda)$ ratios showed a significant increase with the increase in the OC/M_{BC} ratio. The ratios were even higher in Kisai than those in Tokyo (not shown). A significant fraction of the unheated-$b_{abs}(\lambda)$/heated-$b_{abs}(\lambda)$ ratio at low OC/M_{BC} ratio (0.5 or less) may be explained by the absence of the scattering correction (15%). At Gosan, the unheated-$b_{abs}(\lambda)$/heated-$b_{abs}(\lambda)$ ratios was much lower than those in Tokyo even in the high OC/M_{BC} regime. The high OC/M_{BC} air was strongly influenced by the transport from Northeastern China.

If we assume f_{amp} increases with the increase in D_p/D_{BC}, the unheated-$b_{abs}(\lambda)$/heated-$b_{abs}(\lambda)$ ratio should actually be higher at Gosan than in Tokyo (Table 2). Interestingly, the present observations suggest that light absorption by BC did not increase with the increase in D_p/D_{BC}. The cause of this point is discussed more quantitatively in section 6.2.

In rural Guangzhou, the unheated-$b_{abs}(\lambda)$/heated-$b_{abs}(\lambda)$ ratio was more or less similar to that at Gosan. BC mixing state there was not fully understood.

By contrast, heated-$C_{abs}(\lambda)$ was stable between 9.7 and 11.6 $m^2\ g^{-1}$, with an average value of $10.5 \pm 0.7\ m^2\ g^{-1}$. It is very likely that BC in Tokyo, Yufa, and Bangkok in the rainy season was strongly influenced by diesel emissions. The size distribution and $\sigma^*_{abs}(D_{BC}, \lambda)$ of BC emitted from diesel vehicles may vary depending on the types of vehicles and their operating conditions. However, the maximum difference in heated-$C_{abs}(\lambda)$ was within 15%.

The AIT site in Bangkok was occasionally influenced by biomass burning during the dry season, as discussed in section 5.1. We have conducted more detailed analysis of the possible difference of heated-$C_{abs}(\lambda)$ for BC emitted by biomass burning. The largest effect on BC is vehicular emissions, which results in the regular peaks of EC at 0600–0800 LT that can be seen in Figure 6. The effect of biomass burning is most pronounced in winter (December and February) and at 2200-0400 LT. The $b_{abs}(\lambda)$-M_{BC} correlations in different seasons for the whole day, 0600-0800 LT, and 2200-0400 LT are summarized in Table 4, together with the OC/M_{BC} ratios. The average heated-$C_{abs}(\lambda)$ values obtained at different periods given in Table 4 are also plotted versus the average OC/M_{BC} ratio in Figure 9. The largest effect of traffic at 0600-0800 LT in summer is seen by the lowest OC/M_{BC} ratio of 0.9. The largest effect of biomass burning at 2200-0400 LT in winter is reflected in the highest OC/M_{BC} ratio of 3.3. The heated-$C_{abs}(\lambda)$ for OC/M_{BC} ratio close to 1 (fresh BC) was about 9 $m^2\ g^{-1}$ and increased to 10–10.7 $m^2\ g^{-1}$ at OC/M_{BC} ratios greater than 2 (aged BC), although the heated-$C_{abs}(\lambda)$ did not show a monotonic increase with the OC/M_{BC} ratio. It should be noted that the 10% changes in the heated-$C_{abs}(\lambda)$ can also be influenced by the uncertainty of the measurements of M_{BC}, associated with the uncertainty of the EC-OC split depending on the OC/M_{BC} ratio.

Heating of the sample air to 400°C has little effect on the BC mass collected on filters, as discussed in section 3.2. Charring of organic aerosol compounds should also have an insignificant effect on $b_{abs}(\lambda)$ because charred mass was estimated to be insignificant. In fact, we have shown that heated-$C_{abs}(\lambda)$ measured in Tokyo agreed with that measured in Kisai and Gosan to within 11%, despite the significant differences in the D_p/D_{BC} and OOA/M_{BC} ratios. This confirms the limited effects of charring on $b_{abs}(\lambda)$, if it ever occurs for the present heated inlet. Evaporation of volatile aerosol components excludes the necessity of the scattering correction. The effect of SOA is also removed by this technique. All these contribute to the stability of the heated-$C_{abs}(\lambda)$.

The stable heated-$C_{abs}(\lambda)$ value under largely different BC sources, mixing states, and co-existing light-scattering particle concentrations demonstrates the great advantage of using the heated inlet in deriving M_{BC} from $b_{abs}(\lambda)$. The experimentally

TABLE 3
Statistics of the correlation between the absorption coefficient (b_{abs}) and BC mass concentration for heated and unheated inlets at different sites. b_{abs} was measured by either PSAP or COSMOS

Site and period	Regression parameters	Unheated b_{abs} vs. M_{BC}	Heated b_{abs} vs. M_{BC}	Unheated/Heated
RCAST in Tokyo, Summer 2004	Slope ($m^2\ g^{-1}$)	14.97	9.69	1.54
	Intercept (Mm^{-1})	−4.17	1.40	
	r^2	0.89	0.92	
	n	445	450	
CESS in Saitama, Summer 2004	Slope	17.51	10.50	1.67
	Intercept	−1.25	−2.70	
	r^2	0.83	0.87	
	n	24	60	
Gosan on Jeju Island, Spring 2005	Slope	12.32	10.56	1.17
	Intercept	0.54	0.51	
	r^2	0.94	0.94	
	n	366	391	
Rural Guangzhou, Summer 2006	Slope	12.03	9.87	1.22
	Intercept	2.09	4.17	
	r^2	0.96	0.96	
	n	484	485	
Rural Beijing, Summer 2006	Slope	15.71	11.64	1.35
	Intercept	−1.50	−0.94	
	r^2	0.80	0.94	
	n	60	60	
AIT in Bangkok, July–August 2007	Slope	NA	9.6	NA
	Intercept		0.3	
	r^2		0.98	
	n		183	
AIT in Bangkok, November–December 2007	Slope	NA	10.6	NA
	Intercept		3.0	
	r^2		0.93	
	n		1783	
Mean	Slope	14.51	10.35	1.39
Median		14.97	10.50	1.35
S.D.		2.32	0.71	—-

derived heated-$C_{abs}(\lambda)$ value of $10.5 \pm 0.7\ m^2\ g^{-1}$ can be applied to estimate M_{BC} from COSMOS and PSAP observations in urban and remote areas in the fine mode.

5.3. Uncertainty of M_{BC} Derived by the EC-OC Instrument

It is suggested that significant errors of M_{BC} derived from the EC-OC analyzer arise from errors in separating EC and OC (e.g., Boparai et al. 2008), although measurements of total organic carbon (TOC = EC + OC) are sufficiently accurate. Round-robin tests of the EC analysis using different thermal and optical methods showed 1σ differences of 14–24% after selecting reliable measurements (Schmid et al. 2001). The present measurement method is one of the methods used in the above intercomparison. The 22% uncertainty of the present EC measurements was derived from the difference of the EC values obtained by using different protocols. This uncertainty is similar to the variability of EC observed by the above intercomparison. In addition, our recent measurements of M_{BC} by the SP2 in fall 2008 in Tokyo agreed with that by the COSMOS instrument to within about 10% (unpublished data). This, in turn, indicates that the M_{BC} by the EC-OC instrument agrees well with the SP2 measurements, because the heated-$C_{abs}(\lambda)$ value used for the COSMOS is based on the EC measurements, as discussed above. Assuming an uncertainty of M_{BC} of 22%, the absolute uncertainty of the heated-$C_{abs}(\lambda)$ is estimated to be $\pm 2.4\ m^2\ g^{-1}$. It should be noted that this uncertainty is different from the

TABLE 4
Statistics of the correlation between the absorption coefficient and BC mass concentration for heated inlets and mean OC/M_{BC} ratios at Bangkok in different seasons

Site and period	Regression parameters	Heated b_{abs} vs. M_{BC}	Heated b_{abs} vs. M_{BC}	Heated b_{abs} vs. M_{BC}
Local Time		0000-2300	2200-0400	0600-0800
July–August 2007	Slope (m^2 g^{-1})	9.6	10.0	9.02
	Intercept (Mm^{-1})	0.3	–1.2	0.8
	r^2	0.98	0.98	0.98
	OC/M_{BC}	1.7 ± 1.0	2.9 ± 1.5	0.9 ± 0.3
	n	183	55	23
September–November 2007	Slope	9.3	9.8	9.1
	Intercept	0.18	–1.0	0.6
	r^2	0.98	0.98	0.98
	OC/M_{BC}	2.0 ± 1.0	1.8 ± 0.8	1.3 ± 0.6
	n	1461	404	173
December–February 2007–08	Slope	10.6	10.6	10.7
	Intercept	3.0	1.7	0
	r^2	0.93	0.93	0.94
	OC/M_{BC}	3.2 ± 1.4	2.8 ± 1.3	2.3 ± 0.9
	n	1783	509	205
March–May 2008	Slope	10.0	10.0	10.3
	Intercept	–3.9	–1.7	6.5
	r^2	0.85	0.95	0.80
	OC/M_{BC}	3.4 ± 1.7	3.3 ± 1.5	2.2 ± 0.9
	n	827	160	102
Annual 2007–08	Slope	10.8	10.85	11.2
	Intercept	–2.1	–2.3	–7.9
	r^2	0.92	0.95	0.93
	OC/M_{BC}	2.6 ± 1.1	2.5 ± 1.3	1.8 ± 0.9
	n	4210	1130	503

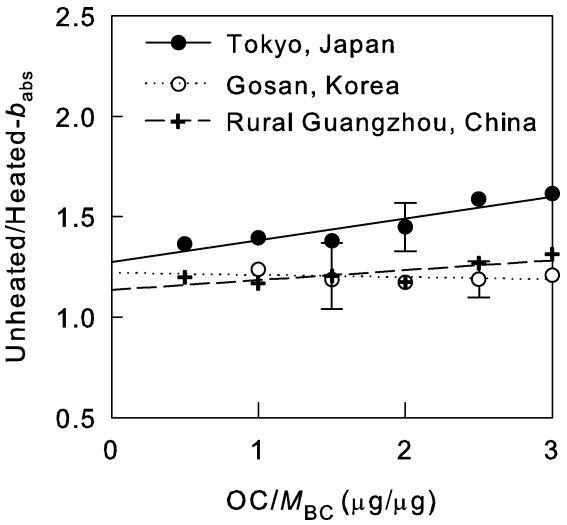

FIG. 8. Median unheated-$b_{abs}(\lambda)$/heated-$b_{abs}(\lambda)$ ratios versus the OC/M_{BC} ratio in Tokyo, in rural Guangzhou, and at Gosan. The bars represent 1-σ ranges.

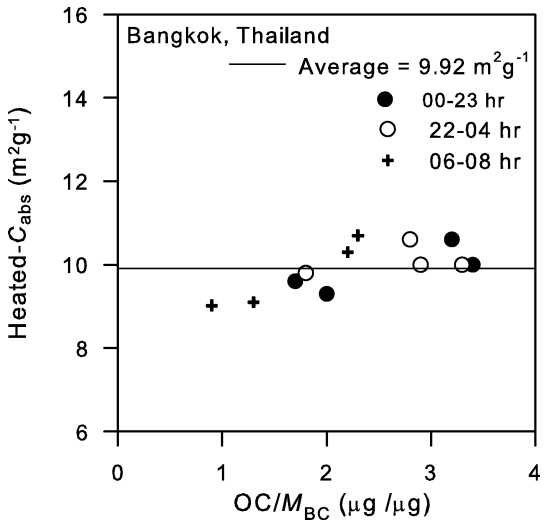

FIG. 9. Heated-$C_{abs}(\lambda)$ plotted versus the mean OC/M_{BC} ratio at different local times and seasons in Bangkok given in Table 4.

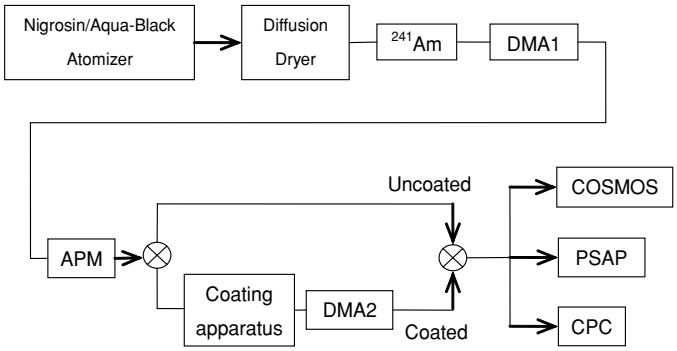

FIG. 10. Instrumental setup for the measurement of $C_{abs}(\lambda)$ of mono-disperse nigrosin particles by COSMOS and PSAP using a tandem differential mobility analyzer (DMA) and aerosol particle mass analyzer (APM). Particle numbers collected by COSMOS and PSAP were measured by a condensation particle counter (CPC). This setup was also used for the measurement of $C_{abs}(\lambda)$ for mono-disperse aqua-black particles coated by oleic acid.

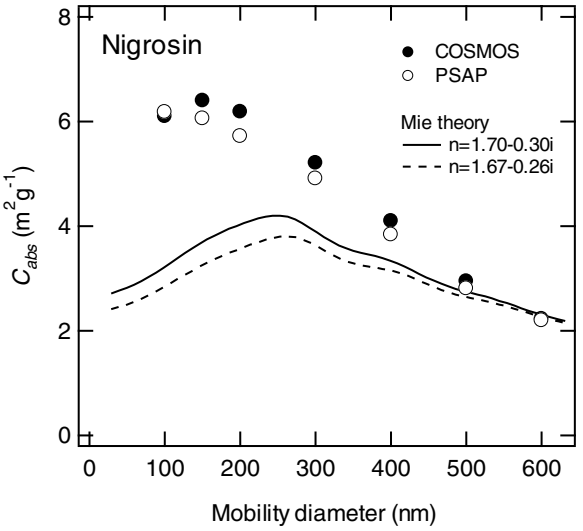

FIG. 11. $C_{abs}(\lambda)$ of nigrosin particles measured by COSMOS and PSAP with an unheated inlet and the calculated $C^*_{abs}(\lambda)$ for $n = 1.70 - 0.30i$ and $n = 1.67 - 0.26i$ at $\lambda = 565$ nm.

variability of the heated-$C_{abs}(\lambda)$ (± 0.7 m^2 g^{-1}) we discussed thus far.

6. LABORATORY MEASUREMENTS OF $C_{abs}(\lambda)$

6.1. Size Dependence of $C_{abs}(\lambda)$ for Nigrosin

The ratio of the heated-$C_{abs}(\lambda) = 10.5 \pm 0.7$ m^2 g^{-1} to the calculated $C^*_{abs}(\lambda) = 5.7 \pm 0.3$ m^2 g^{-1} is about 1.8. A ratio significantly higher than 1 can be due to the uncertainty in the absolute accuracies of M_{BC} and/or $b_{abs}(\lambda)$. It is unlikely that the errors in M_{BC} explain the high heated-$C_{abs}(\lambda)/C^*_{abs}(\lambda)$ ratio, as discussed in section 5.3. It is very likely that the absolute value of $b_{abs}(\lambda)$ was overestimated. The major uncertainty in $b_{abs}(\lambda)$ is caused by the uncertainties in f_{fil}, because $b_0(\lambda)$ is generally accurate to within about 5% for sufficiently high M_{BC}. We consider that the major error in f_{fil} is due to its size dependence, which has not been taken into account. We investigated this effect by laboratory experiments using size selected nigrosin ($C_{48}N_9H_{51}$) particles, as detailed below.

Thus far, we used Equation (6) for f_{fil} as a factor to correct for the effect of multiple scattering. Bond et al. (1999) derived f_{fil} using poly-disperse particles in the fine mode generated using a solution of nigrosin dye. Precise size distributions were not given in their pioneering work, although nigrosin particles were observed in the size range of 100–500 nm by transmission electron microscopy. However, f_{fil} can change with BC diameter, because smaller BC particles penetrate deeper in filter fibers, causing greater light absorption.

In order to assess this effect, we measured $C_{abs}(\lambda)$ as a function of the diameter of nigrosin particles ($D_{nigrosin}$) by generating mono-disperse nigrosin particles. We used nigrosin (Sigma-Aldrich Co.) particles because they are spherical and their refractive index is relatively well known. The configuration of the experiments is shown in Figure 10. Nigrosin particles generated by an atomizer were passed through the tandem DMA and aerosol particle mass analyzer (APM) system to supply nearly mono-disperse particles to COSMOS and PSAP. This system, including the width of the DMA-APM mass filter, is described in detail by Moteki and Kondo (2007). $b_0(\lambda)$ was measured by the photometers operated at a flow rate of about 0.3 STP liter min^{-1}. Then $b_0(\lambda)$ was converted to $b_{abs}(\lambda)$ using Equation (6). The number concentration of nigrosin particles (N) was determined from the particle numbers measured by the CPC. The average mass ($m_{nigrosin}$) of individual particles was measured by the APM. $M_{nigrosin} = N \times m_{nigrosin}$ was used to derive $C_{abs}(\lambda)$. $C_{abs}(\lambda)$ is identical to heated-$C_{abs}(\lambda)$, because the nigrosin particles were uncoated for this experiment.

The measured $C_{abs}(\lambda)$ at each mobility diameter are shown in Figure 11 for $D_{nigrosin}$ between 100 and 600 nm. In this case, the mobility diameter and mass equivalent diameter are identical, because nigrosin particles are spherical. $C^*_{abs}(\lambda)$ was calculated using Mie theory for $n = 1.70 - 0.30i$ (Lack et al. 2006) and $n = 1.67 - 0.26i$ (Garvey and Pinnick 1983) at $\lambda = 565$ nm and is shown in Figure 11 for comparison. $C_{abs}(\lambda)$ was much larger than $C^*_{abs}(\lambda)$, especially at $D_{nigrosin}$ smaller than 300 nm.

The $C_{abs}(\lambda)/C^*_{abs}(\lambda)$ ratios are shown in Figure 12 for more quantitative analysis. The ratio was close to unity and increased with decreasing $D_{nigrosin}$. It was as high as 1.4–1.9 at $D_{nigrosin} =$ 100–200 nm. It should be noted that the median mass diameter of BC mass is about 150–200 nm in ambient air, as discussed in section 4. These results indicate that Equation (6) largely underestimates f_{fil} at $D_{nigrosin} < 500$ nm. If this is taken into account, the heated-$C_{abs}(\lambda)/C^*_{abs}(\lambda)$ ratio will become much closer to unity. For a more quantitative estimate, the BC size distribution has to be considered.

It is likely that the increase in f_{fil} values at smaller BC is due to its deeper penetration into the filter fibers. BC located

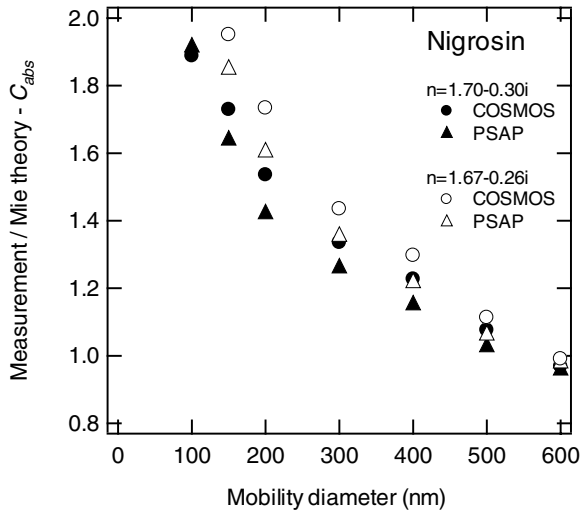

FIG. 12. $C_{abs}(\lambda)/C^*_{abs}(\lambda)$ ratios for nigrosin particles. $C_{abs}(\lambda)$ was measured by COSMOS and PSAP. $C^*_{abs}(\lambda)$ was calculated by Mie theory assuming $n = 1.67 - 0.24i$ and $n = 1.70 - 0.30i$.

deeper in the filter cause higher absorption due to a stronger effect of multiple scattering. f_{fil} may increase with the increase in the flow rate of the photometers, because BC particles may be deposited at locations deeper in the filter at higher flow rates. However, this point was not examined in the present work.

6.2. Amplification of Light Absorption by BC Coating

We showed that the unheated-$b_{abs}(\lambda)$/heated-$b_{abs}(\lambda)$ ratios at Gosan were lower than those in Tokyo and Kisai despite the larger D_p/D_{BC} ratios. For further quantification, we conducted laboratory experiments to measure the amplification of light absorption by coating carbon black (Aqua-Black 162, Tokai Carbon Co., Ltd., Tokyo, Japan) particles at $D_{BC} = 154$ nm with oleic acid using the set-up shown in Figure 10. Aqua-Black 162, suspended in water, is composed of aggregates of primary particles with diameters smaller than 20 nm. Oleic acid is liquid at room temperatures. The apparatus for organic coating is described in detail by Moteki and Kondo (2007). $b_{abs}(\lambda)$ was measured by the COSMOS and PSAP. $C_{abs}(\lambda)$ for coated BC was derived in the same way as described in section 6.1.

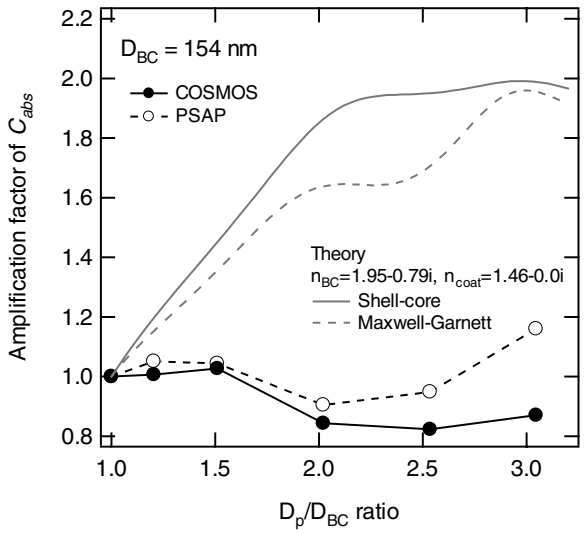

FIG. 13. Amplification factors of $C_{abs}(\lambda)$ of Aqua-Black 162 by organic coating measured by COSMOS and PSAP. The amplification factors of $C^*_{abs}(\lambda)$ calculated by using shell-core and Maxwell-Garnet models are also shown.

The $C_{abs}(\lambda)$ values relative to that for uncoated BC ($D_p/D_{BC} = 1$), namely the amplification factors, are shown in Figure 13 as a function of the D_p/D_{BC} ratio. This figure also shows the calculated amplification factor for $C^*_{abs}(\lambda)$ by using shell-core (Bohren and Huffman 1983) and Maxwell-Garnet (Moteki and Kondo 2008) models for comparison. For these calculations, we used refractive indices $n_{BC} = 1.95 - 0.79i$ for black carbon (Bond and Bergstrom 2006) and $n_{coat} = 1.46 - 0.0i$ for oleic acid (Moteki and Kondo 2008).

Very unexpectedly, the measured $C_{abs}(\lambda)$ showed little increase at a D_p/D_{BC} ratio less than 1.5 and it even showed decreases at D_p/D_{BC} ratios of 2.0–2.5. The observed absence of the amplification is very different from the results for airborne BC particles obtained by laboratory experiments (Schnaiter et al. 2005). The optical models shown in Figure 13 also predict amplification factors of about 2 at $D_p/D_{BC} > 2$.

The lack of amplification indicates the existence of compensating factors. Light absorption by BC should be enhanced by internal mixing, as predicted by the optical models. On the other hand, the growth of D_p (larger D_p/D_{BC} ratio) leads to a shallower penetration depth into the filter fibers of the coated BC particles. This may compensate for the amplification of light absorption by internally mixed BC. This mechanism is consistent with the size dependence of f_{fil} discussed in section 6.1. Another possibility is that that the coating by oleic acid is removed upon impaction of coated BC particles on filter fibers. If oleic acid was separated with BC cores and coats the filter fibers (Subramanian et al. 2007), it should have led to enhanced absorption, similarly to the externally mixed OA. At least, this mechanism will not explain the slight decrease in the amplification factor at $D_p/D_{BC} > 2$.

These results suggest that f_{fil} and f_{amp} are coupled in a complex way. Causing a further complication, external mixing of SOA increases light absorption (Cappa et al. 2008), although internal mixing of SOA should have little or even a negative effect. The lack of the amplification by internally mixed BC at Gosan is consistent with the laboratory experiments. On the other hand, the photo-absorption increased with the OC/M_{BC} ratio in Tokyo, where the degree of internal mixing was relatively lower. It is possible that externally mixed SOA caused the increase in absorption. Quantitative interpretation of these data requires calculations to fully take into account the relevant parameters, including size distribution of BC, D_p/D_{BC} ratio as a function of D_{BC}, and externally mixed OA. Considering these, it is concluded that the difference between the heated and unheated absorption measurements cannot be translated to

absolute BC absorption (heated) and BC absorption coated in a scattering layer (unheated).

6.3. Effect of the Laboratory Data on M_{BC} Derived by Photo-Absorption

The absolute uncertainty in f_{fil} given by Equation (6) does not introduce any additional uncertainty in deriving M_{BC} as long as heated-$C_{abs}(\lambda) = 10.5 \pm 0.7$ m^2 g^{-1} is used together with this equation a directly measured A and V values for Equation (4). Even if a size-dependent f_{fil} is introduced in future studies, the heated-$C_{abs}(\lambda)$ value obtained by the present study can be modified proportionally for the estimate of M_{BC}.

As discussed above, the heated-$C_{abs}(\lambda)$ value for COSMOS and PSAP derived here is for poly-disperse BC particles, commonly encountered in the atmosphere. For mono-disperse BC particles or BC particles with size distributions very different from those discussed here, the heated-$C_{abs}(\lambda)$ is significantly different from the present value. For such specific studies, a size-dependent $C_{abs}(\lambda)$ is required.

7. SUMMARY AND CONCLUSIONS

Light absorption by BC collected on filters has been widely used for the estimation of the mass concentration of BC (M_{BC}). However, accurate determination of M_{BC} has been very difficult due to the observed large variability in the mass absorption cross sections ($C_{abs}(\lambda)$). Coating of BC by volatile compounds and the co-existence of light-scattering particles can greatly contribute to the variation in $C_{abs}(\lambda)$. In order to overcome this difficulty and enable accurate measurements of M_{BC}, volatile aerosol components need to be removed before BC particles are collected on filters. For this purpose we used an inlet section heated at 400°C with a residence time of about 0.3 s. The inlet heated to 400°C was found to vaporize almost completely sulfate, nitrate, ammonium, and organics in ambient air in Tokyo by measurements using Q-AMS. The vaporization temperature of sulfate was also consistent with that measured in the laboratory. We observed no detectable effect of re-condensation of vaporized compounds. No detectable loss of BC mass was observed by this heating. Consistently, the mass concentrations of non-volatile cores extracted by the heating agreed with the M_{BC} measured by an EC-OC analyzer based on the NIOSH-TOT protocol to within 10% at RCAST in Tokyo.

Simultaneous measurements of absorption coefficients ($b_{abs}(\lambda)$) by PSAP and COSMOS together with M_{BC} by the EC-OC analyzer were made to determine $C_{abs}(\lambda)$ in Tokyo and Kisai (Saitama) in Japan, Gosan in Korea, Backgarden (PRD) and Yufa (Beijing) in China, and AIT (Bangkok) in Thailand. The total aerosol mass concentrations, OOA/M_{BC}, OC/M_{BC}, mixing state (D_p/D_{BC}), and types of BC sources (anthropogenic versus biomass burning) showed large variability among these sites. The unheated-$C_{abs}(\lambda)$ showed a larger variability (about 40%) than those for heated-$C_{abs}(\lambda)$ (about 10%). Observations of $b_{abs}(\lambda)$ in Tokyo and at Gosan suggest that light absorption by BC did not increase with the increase in D_p/D_{BC}. Heated-$C_{abs}(\lambda)$ was stable between 9.6 and 11.6 m^2 g^{-1} with an average value of 10.5 ± 0.7 m^2 g^{-1} at $\lambda = 565$ nm. The absolute uncertainty of the heated-$C_{abs}(\lambda)$ was estimated to be ± 2.4 m^2 g^{-1} by considering the uncertainty of M_{BC}.

In Bangkok, the heated-$C_{abs}(\lambda)$ of fresh BC was lower by about 10% than that of aged BC, although this difference is within the uncertainty of the M_{BC} measurement. The stable heated-$C_{abs}(\lambda)$ value under the different physical and chemical conditions and for different types of BC sources provides a firm basis for its use in estimating BC mass concentrations in the fine mode with an accuracy of about 10% by using COSMOS and PSAP.

The ratio of the heated-$C_{abs}(\lambda) = 10.5 \pm 0.7$ m^2 g^{-1} to the calculated $C^*_{abs}(\lambda) = 5.7 \pm 0.3$ m^2 g^{-1} was about 1.8. We measured $C_{abs}(\lambda)$ as a function of $D_{nigrosin}$ using COSMOS and PSAP by generating mono-disperse nigrosin particles in the laboratory. The $C_{abs}(\lambda)/C^*_{abs}(\lambda)$ ratios were close to unity at a $D_{nigrosin}$ of 600 nm and increased with decreasing $D_{nigrosin}$ reaching as high as 1.4–1.9 at $D_{nigrosin} = 100$–200 nm. These results indicate that f_{fil} given by Equation (6) largely underestimates f_{fil} at these diameters. It is likely that the increase in f_{fil} values at smaller BC is due to its deeper penetration into filter fibers. If this is taken into account, the heated-$C_{abs}(\lambda)/C^*_{abs}(\lambda)$ ratio will become much closer to unity. The absolute uncertainty in f_{fil} given by Equation (6) shown here does not lead to additional uncertainty in deriving M_{BC} as long as heated-$C_{abs}(\lambda) = 10.5 \pm 0.7$ m^2 g^{-1} is used together with this equation and directly measured A and V values for Equation (4).

We also measured the amplification of light absorption by coating carbon black particles at $D_{BC} = 154$ nm with oleic acid, followed by collection on filters of the COSMOS and PSAP. Very unexpectedly, the measured $C_{abs}(\lambda)$ showed little increase at a D_p/D_{BC} ratio less than 1.5 and it even showed decreases at D_p/D_{BC} ratios of 2.0–2.5. The larger D_p/D_{BC} ratio may lead to shallower penetration of the coated BC particles into filter fibers, compensating for amplification of light absorption by internally mixed BC. This explains the insensitivity of light absorption by BC to the increase in D_p/D_{BC} observed at Gosan. These results clearly demonstrate that the difference between the heated and unheated absorption measurements cannot be translated to absolute BC absorption (heated) and BC absorption coated in a scattering layer (unheated). The present results suggest the necessity of careful examinations of the filter-based BC measurements made in the past and those currently underway.

REFERENCES

Ackerman, A. S., Toon, O. B., Stevens, D. E., Heymsfield, A. J., Ramanathan, V., and Welton, E. J. (2000). Reduction of Tropical Cloudiness by Soot, *Science* 288:1042–1047.

Arnott, W. P., Moosmuller, H., Sheridan, P. J., Ogren, J. A., Raspet, R., Slaton, W. V., Hand, J. L., Kreidenweis, S. M., and Collett, J. L. (2003). Photoacoustic

and Filter-Based Ambient Aerosol Light Absorption Measurements: Instrument Comparisons and the Role of Relative Humidity, *J. Geophys. Res.* 108 (D1):4034, doi: 10.1029/2002JD002165.

Birch, M. E., and Cary, R. A. (1996). Elemental Carbon-Based Method for Monitoring Occupational Exposures to Particulate Diesel Exhaust, *Aerosol Sci. Technol*. 25:221–241.

Bohren, C. F., and Huffman, D. R. (1983). *Absorption and Scattering of Light by Small Particles*, John Wiley & Sons, Inc.

Bond, T. C., and Bergstrom, R. W. (2006). Light Absorption by Carbonaceous Particles: An Investigative Review, *Aerosol Sci. Technol.* 40:27–67.

Bond, T. C., Anderson, T. L., and Campbell, D. (1999). Calibration and Intercomparison of Filter-Based Measurements of Visible Light Absorption by Aerosols, *Aerosol Sci. Technol.* 30:582–600.

Boparai, P., Lee, J., and Bond, T. C. (2008). Revisiting Thermal-Optical Analyses of Carbonaceous Aerosol Using a Physical Model, *Aerosol Sci. Technol.* 40:930–948.

Cappa, C. D., Lack, D. A., Burkholder, J. B., and Ravishankara, A. R. (2008). Bias in Filter-Based Aerosol Light Absorption Measurements Due to Organic Aerosol Loading: Evidence from Laboratory Measurements, *Aerosol Sci. Technol.* 42: 1022–1032.

Chou, C. C. K., Chen, W. N., Chang, S. Y., Chen, T. K., and Huang, S. H. (2005). Specific Absorption Cross-Section and Elemental Carbon Content of Urban Aerosols, *Geophys. Res. Lett.* 32(2): L21808, doi: 10.1029/2005GL024301.

Clarke, A. D., and Noone, J. (1985). Measurements of Soot Aerosol in Arctic Snow, *Atmos. Environ.* 19:2045–2054.

Clarke, A. D., Ahlquist, N. C., and Covert, D. S. (1987). The Pacific Marine Aerosol: Evidence for Natural Acid Sulfates, *J. Geophys. Res.* 92: 4179–4190.

Crutzen, P. J., and Andreae, M. O. (1990). Biomass Burning in the Tropics: Impact on Atmospheric Chemistry and Biogeochemical Cycles, *Science* 250:1669–1678.

Fuller, K., Malm, W. C., and Kreidenweis, S. M. (1999). Effects of Mixing on Extinction by Carbonaceous Particles, *J. Geophys. Res.* 104(D13):15941–15954.

Gao, R. S., Schwarz, J. P., Kelly, K. K., Fahey, D. W., Watts, L. A., and Thompson, T. L. (2007). A Novel method for Estimating Light-Scattering Properties of Soot Aerosols Using a Modified Single-Particle Soot Photometer, *Aerosol Sci. Technol.* 4:125–135.

Garland, R. M., Yang, H., Schmid, O., Rose, D., Nowak, A., Achtert, P., Wiedensohler, A., Takegawa, N., Kita, K, Miyazaki, Y., Kondo, Y., Hu, M., Shao, M., Zeng, L. M., Zhang, Y. H., Andreae, M. O., and Pöshl, U. (2008). Aerosol Optical Properties in a Rural Environment Near the Mega-City Guangzhou, China: Implications for Regional Air Pollution, Radiative Forcing, and Remote Sensing, *Atmos. Chem. Phys.* 8:1–26.

Garvey, D. M., and Pinnick, R. G. (1983). Response Characteristics of the Particle Measuring Systems Active Scattering Aerosol Spectrometer Probe (ASASP-X), *Aerosol Sci. Technol.* 2:477–488.

Han, S., Kondo, Y., Takegawa, N., Miyazaki, Y., Oshima, N., Hu, M., Lin, P., Deng, Z., Zhao, Y., and Sugimoto, N. (2009). Temporal Variations of Elemental Carbon in Beijing, submitted to *Geophys. Res*.

Hansen, J., and Nazarenko, L. (2004). Soot Climate Forcing via Snow and Ice Albedos, *Proc. Natl. Ac. Sci.* 101:423–428.

Hansen, J., Sato, M., and Ruedy, R. (1997). Radiative Forcing and Climate Response, *J. Geophys. Res.* 102:6831–6864.

Hitzenberger, R., Jennings, S. G., Larson, S. M., Dillner, A., Cachier, H., Galambos, Z., Rouc, A., and Spain, T. G. (1999). Intercomparison of Measurement Methods for Black Carbon Aerosols, *Atmos. Environ*. 33(17):2823–2833.

Horvath, H. (1997). Experimental Calibration for Aerosol Light Absorption Measurements Using the Integrating Plate Method-Summary of the Data, *J. Aerosol Sci.* 28(7):1149–1161.

Huffman, J. A., Ziemann, P. J., Jayne, J. T., Worsnop, D. R., and Jimenez, J. L. (2008). Development and Characterization of a Fast-Stepping/Scanning Thermodenuder for Chemically-Resolved Aerosol Volatility Measurements, *Aerosol Sci. Technol.* 42:395–407.

IPCC (2007). *Climate Change 2007: The Physical Science Basis. Contribution of Working Group I to the 4th Assessment Report of the IPCC*. Cambridge University Press, Cambridge, UK.

Jayne, J. T., Leard, D. C., Zhang, X. F., Davidovits, P., Smith, K. A., Kolb, C. E., and Worsnop, D. R. (2000). Development of an Aerosol Mass Spectrometer for Size and Composition Analysis of Submicron Particles, *Aerosol Sci. Technol.* 33:49–70.

Kim Oanh, N. T., Reutergardh, L. B., Dung, N. T., Yu, M. H., Yao, W. X., and Co, H. X. (2000). Polycyclic Aromatic Hydrocarbons in the Airborne Particulate Matter at a Location 40 km North of Bangkok, Thailand, *Atmos. Environ*. 34:4557–4563.

Kondo, Y., Komazaki, Y., Miyazaki, Y., Moteki, N., Takegawa, N., Kodama, D., Deguchi, S., Nogami, M., Fukuda, M., Miyakawa, T., Morino, Y., Koike, M., Sakurai, H., and Ehara, K. (2006). Temporal Variations of Elemental Carbon in Tokyo, *J. Geophys. Res.* 111:D12205, doi:10.1029/2005JD006257.

Kondo, Y., Miyazaki, Y., Takegawa, N., Miyakawa, T., Weber, R. J., Jimenez, J. L., Zhang, Q., and Worsnop, D. R. (2007). Oxygenated and Water-Soluble Organic Aerosols in Tokyo, *J. Geophys. Res*., 112, D01203, doi:10.1029/2006JD007056.

Kondo, Y., Morino, Y., Fukuda, M. Miyazaki, Y., Takegawa, N., Kanaya, Y., Tanimoto, H., McKenzie, R., Johnston, P., Blake, D. R., and Murayama, T. (2008). Formation and Transport Oxidized Reactive Nitrogen, Ozone, and Secondary Organic Aerosol in Tokyo, *J. Geophys. Res.*, 113, D21310, doi:10.1029/2007JD010134.

Kuwata, M., and Kondo, Y. (2008). Dependence of Size-Resolved CCN Spectra on the Mixing State of Non-Volatile Cores Observed in Tokyo, *J. Geophys. Res.* 113:doi:10.1029/2007JD009761.

Kuwata, M., Kondo, Y., Mochida, M., Takegawa, N., and Kawamurra, K. (2007). Dependence of CCN Activity of Less Volatile Particles on the Amount of Coating Observed in Tokyo, *J. Geophys. Res.* 112: D11207, doi:10.1029/2006JD007758.

Kuwata, M., Kondo, Y., Miyazaki, Y., Komazaki, Y., Kim, J. H., Yum, S. S., Tanimoto, H., and Matsueda, H. (2008). Cloud Condensation Nuclei Activity at Jeju Island, Korea in Spring 2005, *J. Atmos. Chem. Phys.* 8:2933–2948.

Lack, D. A., Lovejoy, E. R., Baynard, T., Petterson, A., and Ravishankara, A. R. (2006). Aerosol Absorption Measurement Using Photoacoustic Spetroscopy: Sensitivity, Calibration, and Uncertainty Developments, *Aerosol Sci. Technol.* 40:697–708.

Lack, D. A., Cappa, C. D., Covert, D. S., Baynard, T., Massoli, P., Sierau, B., Bates, T. S., Quinn, P. K., Lovejoy, E. R., and Ravishankara, A. R. (2008). Bias in Filter-Based Aerosol Light Absorption Measurements Due to Organic Aerosol Loading: Evidence from Ambient Measurements, *Aerosol Sci. Technol.* 42:1033–1041.

Lighty, J. S., Veranth, J. M., and Sarofim, A. F. (2000). Combustion Aerosols: Factors Governing Their Size and Composition and Implications to Human Health, *J. Air Waste Manage. Assoc.* 50:1565–1618.

Liousse, C., Cachier, H., and Jennings, S. G. (1993). Optical and Thermal Measurements of Black Carbon Aerosol Content in Different Environments: Variation of the Specific Attenuation Cross Section, *Atmos. Environ.* 27A(8):1203–1211.

Martins, J. V., Artaxo, P., Liousse, C., Reid, J. S., Hobbs, P. V., and Kaufman, Y. J. (1998). Effects of Black Carbon Content, Particle, and Mixing on Light Absorption by Aerosols from Biomass Burning in Brazil, *J. Geophys. Res.* 103(D24):10332041–32050.

Mikhailov, E. F., Vlasenko, S. S., Podgorny, I. A., Ramanathan, V., and Corrigan, C. E. (2006). Optical Properties of Soot–Water Drop Agglomerates: An Experimental Study, *J. Geophys. Res.* 111:D07209, doi:10.1029/2005JD006389.

Miyakawa, T., Takegawa, N., and Kondo, Y. (2008). Photochemical Evolution of Submicron Aerosol Chemical Composition in the Tokyo Megacity Region in Summer, *J. Geophys. Res.* 113:D14304, doi:10.1029/2007JD009493.

Miyazaki, Y., Kondo, Y., Han, S., Koike, M., Kodama, D., Komazaki, Y., Tanimoto, H., and Matsueda, H. (2007). Chemical Characteristics of

Water-Soluble Organic Carbon in the Asian Outflow, *J. Geophys. Res.* 112: D22S30, doi:10.1029/2007JD009116.

Miyazaki, Y., Kondo, Y., Sahu, L. K., Imaru, J., Fukushima, N., and Kanno, A. (2008). Performance of a Newly Designed Continuous Soot Monitoring System (COSMOS), *J. Env. Monit.* doi:10.1039/b806957c.

Moteki, N., and Kondo, Y. (2007). Effects of Mxing Sate on Back Crbon Masurement by Laser-Induced Incandescence, *Aerosol Sci. Technol.* 41:398–417.

Moteki, N., and Kondo, Y. (2008). Method to Measure Time-Dependent Scattering Cross Sections of Particles Evaporating in a Laser Beam, *J. Aerosol. Sci.* 39:348–364.

Moteki, N., Kondo, Y., Miyazaki, Y., Takegawa, N., Komazaki, Y., Kurata, G., Shirai, T., Blake, D. R., Miyakawa, T., and Koike, M. (2007). Evolution of Mixing State of Black Carbon Particles: Aircraft Measurements over the Western Pacific in March 2004, *Geophys. Res. Lett.* 34:L11803, doi: 10.1029/2006GL028943.

Novakov, T., and Corrigan, C. E. (1995). Thermal Characterization of Biomass Smoke Particles, *Mikrochim. Acta* 117(1–2):157–166.

Paulsen, D., Weingartner, E., Rami Alfarra, M., and Baltensperger, U. (2006). Volatility Measurements of Photochemically and Nebulizer-Generated Organic Aerosol Particles, *J. Aerosol. Sci.* 37:1025–1051.

Petzold, A., Kopp, C., and Niessner, R. (1997). The Dependence of the Specific Attenuation Cross-Section on Black Carbon Mass Fraction and Particle Size, *Atmos. Environ.* 31(5):661–672.

Philippin, S., Wiedensohler, A., and Stratmann, F. (2004). Measurements of Non-Volatile Fractions of Pollution Aerosols with an Eight-Tube Volatility Tandem Differential Mobility Analyzer (VTDMA-8), *J. Aerosol Sci.* 35(2):185–203.

Pinnick, R. G., Jennings, S. G., and Fernandez, G. (1987). Volatility of Aerosols in the Arid Southwestern United States, *J. Atmos. Sci*. 44:562–576.

Ramanathan, V., Crutzen, P. J., Kiehl, J. T., and Rosenfeld, D. (2001). Aerosols, Climate, and the Hydrological Cycle, *Science* 294:2119–2124.

Ramanathan, V., Ramana, M. V., Roberts, G., Kim, D., Corrigan, C., Chung, C., and Winker, D. (2007). Warming Trends in Asia Amplified by Bown Cloud Solar Absorption, *Nature* 448:575–579.

Reid, J. S., Hobbs, P. V., Liousse, C., Martins, J. V., Weiss, R. E., and Eck, T. F. (1998). Comparisons of Techniques for Measuring Shortwave Absorption and Black Carbon Content of Aerosols from Biomass Burning in Brazil, *J. Geophys. Res.* 103(D24):32031–32040.

Sahu, L. K., Kondo, Y., Miyazaki, Y., Koike, M., Tanimoto, H., Matsueda, H., Yoon, S. C., and Kim, Y. J. (2008). Anthropogenic Aerosols Observed in Asian Continental Outflow at Jeju Island, Korea in Spring 2005, *J. Geophys. Res.,* in press.

Schmid, H., Laskus, L., Abraham, H. J., Baltensperger, U., Lavanchy, V., Bizjak, M., Burba, P., Cachier, H., Crow, D., Chow, J., Gnauk, T., Even, A., Brink, H. M. T., Giesen, K.-P., Hitzenberger, R., Huegelin, C., Maenhaut, W., Pio, C., Carvalho, A., Putaud, J.-P., Toom-Sauntry, D., and Puxbaum, H. (2001). Results of the "Carbon Conference" International Aerosol Carbon Round Robin Test Stage I. *Atmos. Env.* 35:2111–2121.

Schnaiter, M., Linke, C., Möhler, O., Naumann, K.-H., Saathoff, H., Wagner, R. Schurath, U., and Wehner, B. (2005). Absorption Amplification of Black Carbon Internally Mixed with Secondary Organic Aerosol, *J. Geophys. Res.* 110:D19204, doi:10.1029/2005JD006046.

Schwarz, J. P., Gao, R. S., Spackman, J. R., Watts, L. A., Thomson, D. S., Fahey, D. W., Ryerson, T. B., Peischl, J., Holloway, J. S., Trainer, M., Frost, G. J., Baynard, T., Lack, D. A., de Gouw, J. A., Warnecke, C., and Del Negro, L. A. (2008). Measurement of the Mixing State, Mass, and Optical Size of Individual Black Carbon Particles in Urban and Biomass Burning Emissions, *Geophys. Res. Lett.* 35: L13810, doi:10.1029/2008GL033968.

Sharma, S., Brook, J. R., Cachier, H., Chow, J., Gaudenzi, A., and Li, G. (2002). Light Absorption and Thermal Measurements of Black Carbon in Different Regions of Canada, *J. Geophys. Res.* 107(D24):4771, doi: 10.1029/2002JD002496.

Sheridan, P. J., Arnott, W. P., Ogren, J. A., Andrews, E., Atkinson, D. B., Covert, D. S., Moosmüller, H., Petzold, A., Schmid, B., Strawa, A. W., Varma, R., and Virkkula, A. (2005). The Reno Aerosol Optics Study: An Evaluation of Aerosol Absorption Measurement Methods, *Aerosol Sci. Technol.* 39:1–16.

Shiraiwa, M., Kondo, Y., Moteki, N., Takegawa, N., Miyazaki, Y., and Blake, D. R. (2007). Evolution of Mixing State of Black Carbon in Polluted Air from Tokyo, *Geophys. Res. Lett.* 34:L16803, doi:10.1029/2007GL029819.

Shiraiwa, M., Kondo, Y., Moteki, N., Takegawa, N., Sahu, L. K., Takami, A., Hatakeyama, S., Yonemura, S., and Blake, D. R. (2008). Radiative Impact of Mixing State of Black Carbon Aerosol in Asian Outflow, *J. Geophys. Res.* 113:D24210, doi:1029/2008JD10546.

Slowik, J. G., Cross, E., Han, J.-H., Davidovits, P., Onasch, T. B., Jayne, J. T., Williams, L. R., Canagaranata, M. R., Worsnop, D. R., Chakrabarty, R. K., Mossmüller, H., Arnott, W. P., Schwarz, J. P., Gao, R.-S., Fahey, D. W., Kok, G. L., and Petzold, A. (2007). An Inter-Comparison of Instruments Measuring Black Carbon Content of Soot Particles, *Aerosol Sci. Technol.* 41(3):295–314.

Springston, S. R., and Sedlacek, A. J. (2007). Noise Characteristics of an Instrumental Particle Absorbance Technique, *Aerosol Sci. Technol.* 41:1110–1116.

Streets, D. G., et al. (2003). An Inventory of Gaseous and Primary Aerosol Emissions in Asia in the Year 2000, *J. Geophys. Res.* 108(D21):8809, doi:10.1029/2002JD003093.

Subramanian, R., Roden, C. A., Boparai, P., and Bond, T. (2007), Yellow Beads and Missing Particles: Trouble Ahead for Filter-Based Absorption Measurements, *Aerosol Sci. Technol.* 41:630–637.

Taha, G., Box, G. P., Cohen, D. D., and Stelcer, E. (2007). Black Carbon Measurement Using Laser Integrating Plate Method, *Aerosol Sci. Technol.* 41:266–276.

Takegawa, N., Miyazaki, Y., Kondo, Y., Komazaki, Y., Miyakawa, T., Jimenez, J. L., Jayne, J. T., Worsnop, D. R., Allan, J., and Weber, R. J. (2005). Characterization of an Aerodyne Aerosol Mass Spectrometer (AMS): Long Term Stability and Intercomparison with Other Aerosol Instruments, *Aerosol Sci. Technol.* 39:760–770.

Villani, P., Picard, D., Marchand, N., and Laj, P. (2007). Design and Validation of a 6-Volatility Tandem Differential Mobility Analyzer (VTDMA), *Aerosol Sci. Technol.* 41:898–906.

Virkkula A., Ahlquist, N. C., Covert, D. S., Arnott, W. P., Sheridan, P. J., Quinn, P. K., and Coffman, D. J. (2005). Modification, Calibration and a Field Test of an Instrument for Measuring Light Absorption by Particles, *Aerosol Sci. Technol.* 39:68–83.

Warren, S. G., and Wiscombe, W. J. (1980). A Model for the Spectral Albedo of Snow, II, Snow Containing Atmospheric Aerosol, *J. Atmos. Sci.* 37, 2734–2745.

Yu, J.Z., Xu, J., and Yang, H. (2002). Charring Characteristics of Atmospheric Organic Particulate Matter, *Environ. Sci. Technol.* 36:754–761.

Zhang, R., Khalizov, A. R., Pagels, J., Zhang, D., Xue, H., and McMurry, P. H. (2008). Variability in Morphology, Hygroscopicity, and Optical Properties of Soot Aerosols During Atmospheric Processing, *Proc. Natl. Ac. Sci.* 105 (30):10291–10296.